Single-Detector Polarization-Sensitive Optical Coherence Tomography for Assessment of Rotator Cuff Tendon Integrity

Christopher Rashidifard, BS, Scott Martin, MD, Namita Kumar, MS, Ehsan Azimi, MS, Bin Liu, PhD, and Mark E. Brezinski, MD, PhD

Abstract

This preliminary study assessed trimmed supraspinatus tendons from rotator cuff repairs (RCRs) to compare the samples' surgically cut ends and torn ends with histopathology and polarization-sensitive optical coherence tomography (PS-OCT) imaging. PS-OCT can be used to assess collagen content and organization in birefringent tissue and shows promise in RCR. The data were compared to determine correlations between luminosity measured from histopathology and PS-OCT. Bivariate plots and a simple regression were performed to assess the linearity of the 2 groups, with a predictive value of less than .05 showing significant correlation.

Approximately 50% of the visually inspected supraspinatus tendons acceptable for RCR exhibited collagen depletion when examined by histopathology, compared with PS-OCT. Because a strong correlation in collagen concentrations existed between histopathology and PS-OCT polarized back-reflection intensity, this study established the potential of PS-OCT for clinical use in the assessment of collagen content and organization to improving outcomes in RCR.

Mr. Rashidifard is Research Assistant, Center for Optical Coherence Tomography and Optical Physics, Department of Orthopedic Surgery, Brigham and Women's Hospital, Boston, Massachusetts, and Associate in Orthopedic Surgery, Harvard Medical School, Boston, Massachusetts.
Dr. Martin is Attending Orthopedic Surgeon, Center for Optical Coherence Tomography and Optical Physics, Department of Orthopedic Surgery, Brigham and Women's Hospital, Boston, Massachusetts, and Associate Professor of Orthopedic Surgery, Harvard Medical School, Boston, Massachusetts.
Namita Kumar is Research Assistant, Center for Optical Coherence Tomography and Optical Physics, Department of Orthopedic Surgery, Brigham and Women's Hospital, Boston, Massachusetts.
Ehsan Azimi is Research Assistant, Center for Optical Coherence Tomography and Optical Physics, Department of Orthopedic Surgery, Brigham and Women's Hospital, Boston, Massachusetts, and Associate in Orthopedic Surgery, Harvard Medical School, Boston, Massachusetts.
Dr. Liu is Scientist, Center for Optical Coherence Tomography and Optical Physics, Department of Orthopedic Surgery, Brigham and Women's Hospital, Boston, Massachusetts, and Instructor, Harvard Medical School, Boston, Massachusetts.
Dr. Brezinski is Director, Center for Optical Coherence Tomography and Optical Physics, Department of Orthopedic Surgery, Brigham and Women's Hospital, Boston, Massachusetts, and Professor of Orthopedic Surgery, Harvard Medical School, Boston, Massachusetts.

Address correspondence to: Mark E. Brezinski, MD, PhD, Center for Optical Coherence Tomography and Optical Physics, Department of Orthopedic Surgery, Brigham and Women's Hospital, Boston, MA 02115 (tel, 617-732-6911; fax, 617-525-8356; e-mail, mebrezin@mit.edu).

Full- or partial-thickness tears of rotator cuff tendons (RCTs) are relatively common, occurring in approximately 30% of the population and representing 4.5 million clinic visits and 40,000 surgeries in the United States anually.[1] The most common RCT injury is a supraspinatus tear at the greater humoral tuberosity enthesis.[2-15] Unfortunately, 25% to 60% of repaired RCTs rerupture within 2 years.[16,17] Rotator cuff repairs (RCRs) are performed by flattening a foundation on the greater humoral tuberosity to secure the RCT remnants.[18] Strong evidence suggests that formation of a new fibrocartilage at the enthesis site depends heavily on migration of chondrocytes and plu-

> "The goal was to determine the feasibility of using polarization-sensitive optical coherence tomography as a potential diagnostic tool for assessing tendon collagen."

ripotent mesenchymal cells, from the greater tuberosity into the reattached tendon.[19-21] Although the importance of these migratory cells cannot be underestimated, the integrity of the tendon clearly plays a role in the enthesis process.

The condition of the tendon at the time of repair is likely to affect the success rate; it is hypothesized that reattachment of a degraded tendon can increase the risk for surgical failure.[14,22-23] During surgery, a viable tendon with highly organized type I collagen is an excellent milieu for both suture support and cell migration, even when the matrix is reorganized. Surgeons rely primarily on the visual appearance of the tendon and prior experience with RCRs. However, visually normal but structurally weak collagen-depleted tendon is often used at the reattachment site, leading to reduced tensile strength of the tendon-enthesis interface and a paucity of structure for establishing a strong attachment. Therefore, outcomes of repair would likely improve if the surgeon were to resect the collagen-depleted remnant tendon through appropriate guidance and reattach

highly organized tendon to the bone interface. Aside from postoperative histopathology, evaluations of collagen quantity and organization at reattachment sites are difficult to perform. Computed tomography, magnetic resonance imaging, ultrasonography, and conventional radiography do not detect organized collagen and have limited resolution.[14,24] Optical coherence tomography (OCT), particularly polarization-sensitive OCT (PS-OCT), represents a promising technology for assessing the integrity of tendons in RCRs.[25,26]

OCT is an imaging technology that operates in a way analogous to that of ultrasonography, using infrared light as opposed to acoustical waves. The time it takes light to reflect back, echo delay time, is used to measure distance discrepancies between the sample arm and the reference arm. The intensity of back-reflection is plotted as the function of depth. The beam is then scanned across the sample to create 2- and 3-dimensional (2D, 3D) data sets. OCT has shown tremendous potential for assessing musculoskeletal tissue, particularly tendon collagen organization. OCT can be used to perform optical biopsies, which provide diagnostic information at the level of low-resolution microscopy without tissue destruction. OCT is based on a technique, optical low–coherence interferometry, that has been applied in microelectronic devices and in transparent tissue to measure distances with micrometer resolution. For more than 15 years, our laboratory has worked on developing OCT for imaging nontransparent tissue. This work has included advances in spectroscopic techniques, including PS-OCT and elastography, further refining the ability of OCT to image tissue properties.[23,27-31]

OCT has several advantages over other imaging modalities. First, its resolution is up to 25 times higher than that of anything used in clinical medicine. Second, its 0.043 cm fiberoptic-based endocatheter can be used during diagnostic arthroscopic examinations or surgery with a handheld probe. Third, its data are acquired at a rate faster than video rate, allowing more than 30 high-resolution optical biopsies per second. Fourth, it is compact and portable, and lastly, it can be combined with a range of spectroscopic techniques, including PS-OCT, which can be used to assess organized collagen. Most tissue is not birefringent or sensitive to the polarization state of incident light. For tissue with highly organized collagen, however, the back-reflection intensity varies with the incident light polarization state. As demonstrated in other studies, collagen organization is lost with many pathologic processes, resulting also in loss of polarization sensitivity.[32,33] Strong in vitro correlations have been found between birefringence with PS-OCT images and histopathology of tendon, ligament, cartilage, and arteries.[33-41] In vivo studies have been performed with a handheld probe in open joints in humans and in rats, and ongoing endocatheter-based arthroscopic studies of articular knee cartilage are under way.[32,42,43]

In this article, we introduce a new technology for assessing RCTs. We report on a study in which we examined use of PS-OCT in differentiating non–collagen depleted and collagen-depleted supraspinatus tendon by correlating images with histology. The goal was to determine the feasibility of using PS-OCT as a potential diagnostic tool for assessing tendon collagen. Our long-term objective is to develop real-time PS-OCT assessment of collagen during surgery and potentially improve RCR outcomes.

METHODS AND MATERIALS

To assess the viability of the technology, we obtained resected tendon (portions not used in reattachment) from patients who underwent arthroscopic repair of full-thickness tears of the supraspinatus tendon. Patient selection was not criteria based, but random, and, as this was a technology assessment study, demographic screening was not performed. The orthopedic surgeon, Dr. Martin, resected each supraspinatus tendon section until he felt he had a healthy tendon for reattachment. The proximal end of the resected tendon (distal end of remaining tendon) was considered healthy when it was indistinguishable from the unruptured tendon. These harvested samples were marked and used for in vitro assessment with PS-OCT, with the transected end evaluated as normal and the ruptured end deemed abnormal. The protocol was approved by the institutional review board of Brigham and Women's Hospital.

OCT was performed with a modified swept source system (Thorlabs, Newton, New Jersey), with images captured at a rate of 25 frames per second and a resolution of 1024×512 pixels. The 2D cross-sections were imaged with 15-μm transverse resolution and 12-μm axial resolution. The system (Figure 1) consists of a 10-mW, 1325-nm infrared tunable laser light source at 6-mm coherence length. We added external polarization controllers to the system and polarization rotation was performed through 180° in 2 seconds.[32,33] Seven hundred frames minimum were captured at each site. A site represented either the distal or the proximal portion of the harvested tendon. Both ends of each sample were positioned so that, during OCT imaging, a 2D cross-sectional image would be generated. Because of the polarization rotation, the tendons were imaged at multiple polarization states by the rotating polarization controller, so that the organization of the birefringent collagen could be assessed properly, as previously described. The intensity of birefringence by PS-OCT was determined by measuring the maximum and minimum back-reflection regionally in the tendon, as the polarization controller was rotated through different polarization states. Large variation in back-reflection intensity represents high birefringence, and no change in back-reflection intensity represents low birefringence. Regions of interest (ROI) were defined to standardize the technique. They were defined as the tissue sections 0.5 mm from the transection edge. ROI was 5×3 mm with a pixel density of 10 μm/pixel. Before imaging, ROI were marked
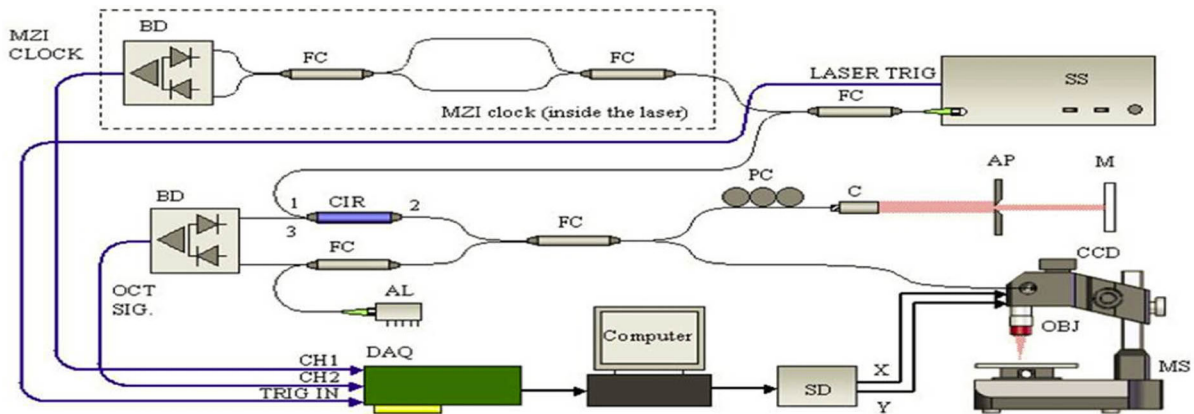
Figure 1. Schematics of optical coherence tomography imaging system (Thorlabs, Newton, New Jersey). SS indicates swept laser source; FC, fiber coupler; PC, polarization controller; CIR, circulator; C, collimator; AP, adjustable pinhole variable attenuator; M, mirror; BD, balanced detector; DAQ, data acquisition board; SD, XY scanners driver; CCD, CCD camera; OBJ, objective; MS, microscope.

with microinjections of dye, which was used to register PS-OCT images with histopathology.

After fixation in 10% formalin for 24 hours, the samples were kept in sterile 7.4-pH phosphate-buffered saline until OCT was performed. This procedure maintains collagen imaging properties in tissue.[44] Imaged RCT samples were processed by routine paraffin embedding and were cross-sectioned at 7 µm. Masson trichrome stain was used to detect any structural abnormalities—this stain is qualitative and is used to ensure no secondary pathology, eg, active inflammation—and picrosirius red stain was used to identify organization, type, and size of collagen fibers.[14,24,27,36-41,45-47]

For the trichrome stain samples, a blue filter (Olympus 45-LBD-1F) was used to improve contrast. For the picrosirius red samples, a polarization filter (Olympus UPOT) was used. The filter was adjusted until the background demonstrated no luminosity, and the position was confirmed by absence of colorization ban artifacts. A high-resolution digital microscope system, an Olympus BX-41 microscope with a Q-color 3-CCD camera (Olympus America, Melville, New York), was used to produce images of the cross-sectioned RCT samples. The picrosirius red-stained RCT sections were then analyzed with Photoshop (Adobe, Sunnyvale, California) for the quantification of collagen types by calculating the mean intensities within the ROI. PS-OCT and picrosirius red stain data are expressed as mean intensity averaged over ROI. PS-OCT images were categorized in the darkest and brightest polarized frames (ie, maximum birefringent changes) as the polarization was rotated. Both of these OCT images were quantified with ImageJ software by calculating mean intensities within the ROI and were expressed as the difference of mean intensities between light and dark polarized frames. Two readers evaluated the data and there were no significant differences in their analysis of the data. Histopathologic analysis and PS-OCT were performed under the supervision of Dr. Brezinski.

Statistical Analysis

Data were compared to determine any correlation between luminosity measured from the picrosirius red–stained regions and the same regions on the OCT images. Bivariate plots were generated, and simple regression analysis was performed to determine the linearity of the 2 groups. Spearman correlation coefficients were calculated. $P<.05$ represented a significant correlation. Predictive value was calculated by separating the data points for the OCT images into thirds, then counting the number of points that fell below the mean of the luminosity values, and then dividing through by the total values in that third. Statistics were calculated with Instat (GraphicsPad Software, San Diego, California).

On the basis of our previous power analysis, if the true correlation is .80, then 9 analyzable samples yield an α of .05. That study yielded a correlation higher than .95, making 9 samples a sufficient power for this study.[47]

Results

The object of this study was to investigate a new approach for evaluating ruptured tendon with PS-OCT in the hope of aiding surgeons during RCT reattachments and repairs. Results from this preliminary study demonstrated the feasibility of a larger in vivo clinical outcome study with demographic information. Tendon integrity
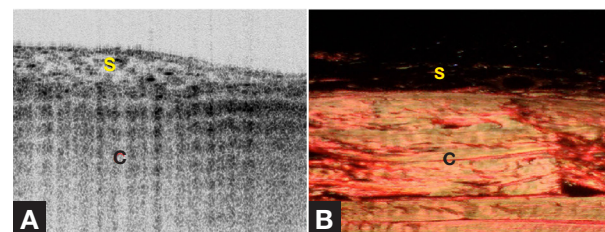

Figure 2. Normal Achilles tendon, one of the most birefringent tissues. (A) Intense banding pattern on optical coherence tomography indicates highly organized collagen. (B) Bright orange on picrosirius red stain histology indicates highly organized type I collagen. S indicates supportive tissue; C, collagen bundle.
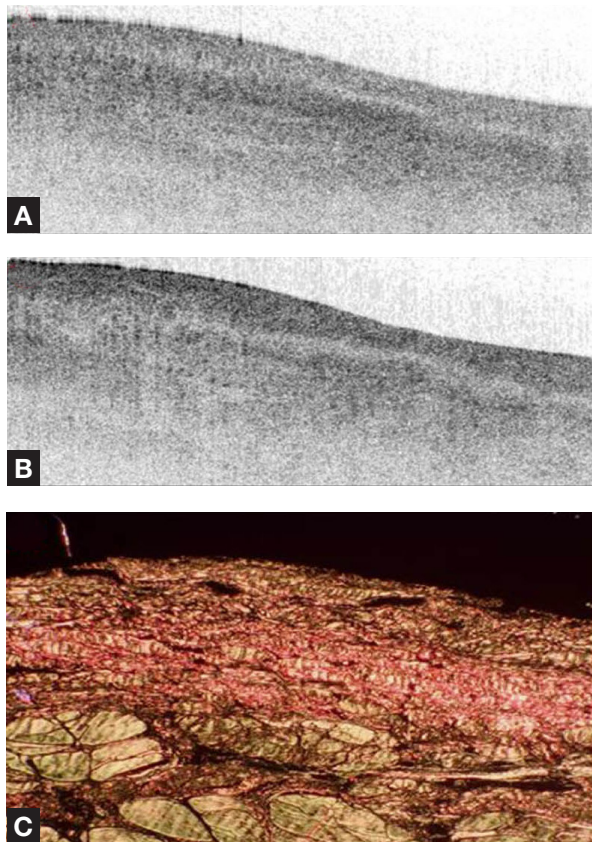
Figure 3. Moderately organized anterior cruciate ligament from geriatric patient post mortem. (A,B) Intense banding pattern is absent, but, as polarization of incident light is rotated, back-reflection intensity changes (does not occur in nonbirefringent tissue). (C) Histology shows relatively organized tendon (even, orangish color).

Figure 4. Very mildly diseased section of supraspinatus tendon. In optical coherence tomography (A), back-reflection intensity changes dramatically between these 2 images, except area with arrow (essentially no change, not birefringent). Even though surgeon deemed sample normal, picrosirius red stain shows dropout of organized collagen (B, arrow) in otherwise healthy collagen. Masson trichrome stain (C) shows fibrocartilage.
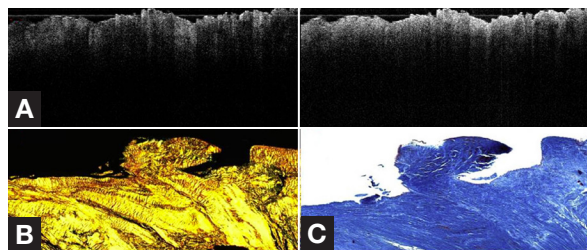
Figure 5. Slightly more diseased section of supraspinatus tendon used for arthroscopic supraspinatus reattachment. Organization is visible on optical coherence tomography, with back-reflection intensity changing dramatically as incident light changes between dark and light polarization (A, left & right). Bright yellow on picrosirius red stain histology shows organized collagen, except at surface, which was partially torn during processing (B). Masson's trichrome shows minimal cartilage (C). Some surface areas did not change as dramatically and therefore showed some degree of disorganization. Had this surface been resected, remaining collagen would be essentially normal.

was initially evaluated by the orthopedic surgeon, Dr. Martin and harvested samples were evaluated by 2 outside readers, whose observations showed no significant differences. Nine supraspinatus tendons were evaluated in this pilot study. Preoperative imaging was not used in this study, as the resolution of current modalities is suboptimal for assessing tissue microstructure.

We used 2 types of healthy, non-RCT tissue with high collagen content to illustrate imaging with high and moderate birefringence. We have worked with both tissue types extensively and feel they are more appropriate for illustrations than RCT, as this article represents our first work with RCT. Figure 2 shows an Achilles tendon with very highly organized, uninjured, type I collagen. In the picrosirius red–stained image (Figure 2B), the sample is bright and yellow-orange below the superficial supportive tissue, consistent with highly organized, type I collagen. The banding patterns on the OCT image result from the rapid rotation of the polarization state of light traveling through the birefringent (polarized) tissue.

Figure 3 illustrates the healthy, yet slightly less organized, collagen structure in an anterior cruciate ligament. The less defined surface collagen has a yellow-reddish color, but the deeper portions of the
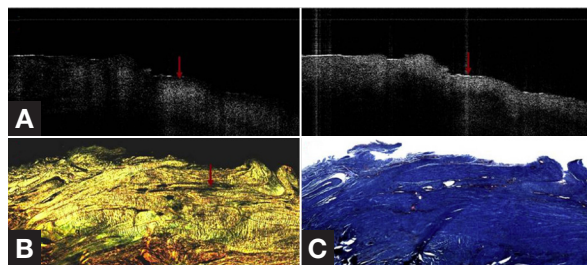
ligament have more defined bundles and are yellowish. As the collagen is not as well organized as the collagen in the Achilles tendon in Figure 2, banding is not as obvious. However, changing the polarization state of the source, or the reference arm, changes the intensity of tissue back-reflection; this does not occur with unpolarized tissue.

Therefore, the principles are as follows: (1) with highly birefringent tissue, intense banding occurs; and (2) with moderately birefringent tissue, birefringence is measured by changing the polarization state of the beam.

A mildly diseased section of supraspinatus tendon is shown in Figure 4. Although the surgeon deemed this sample normal, picrosirius red stain showed a dropout of organized collagen (Figure 4B, arrow) with otherwise healthy tissue. Trichrome stain (Figure 4C) showed that the area is fibrocartilage. On OCT images, back-reflection intensity changed dramatically between the 2 images, except in the area indicated by the arrow, where there was essentially no change.

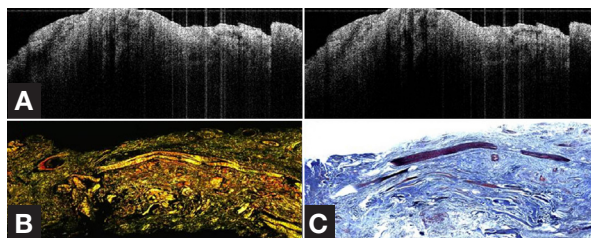Figure 5 shows a slightly more diseased section of supraspinatus tendon used for arthroscopic supraspi-

Figure 6. On visual inspection, supraspinatus tendon sample appeared to be normal and appropriate for reattachment; optical coherence tomography (OCT) and histopathology showed obviously diseased section depleted of collagen. OCT suggests that no significant intensity variation in back-reflection occurs when polarization state is manipulated (A). Picrosirius red stain shows minimal areas of organized type I collagen and a relatively green hue suggestive of structurally weak type III collagen in tendon (B).
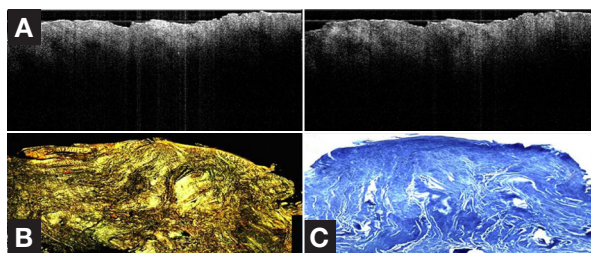

Figure 7. (A) Optical coherence tomography shows essentially no change in polarization, consistent with poorly organized collagen in this section, which was deemed normal on visual inspection. Figure 8 shows similar results. (B, C) Masson trichrome–stained sections are consistent with fibrocartilage, and picrosirius red–stained sections show lack of organized collagen bundles, even though collagen is abundant.
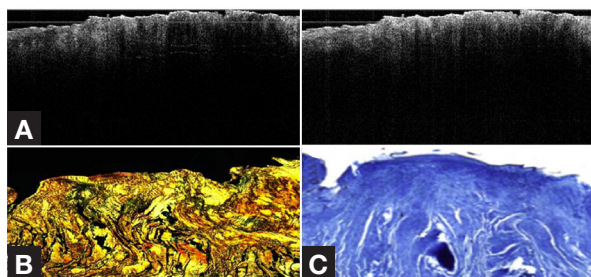

Figure 8. Similar to Figure 7, except fibrocartilage is denser.

natus reattachment. Picrosirius red stain showed bright yellow organized collagen except at the surface, which was partially torn during processing (Figure 5B). The organization is visible on the OCT image, as back-reflection intensity changes dramatically with polarization changes of the incident light between dark and light polarizations (Figure 5A, left & right). However, areas of the surface did not change as dramatically, demonstrating some degree of disorganization.

Figure 6 shows a collagen-depleted section of tendon, and Figures 7 and 8 show sections in which fibrocartilage (disorganized) is present. Figure 6 shows a diseased supraspinatus tendon deemed normal at time
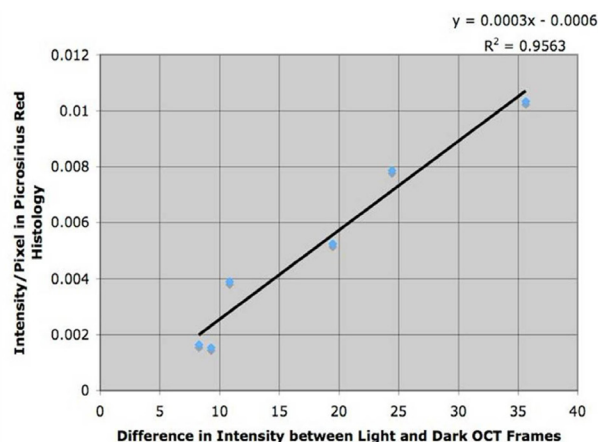

Figure 9. Plot of collagen intensity (picrosirius red stain) against change in incident light polarization on optical coherence tomography shows linear correlation (coefficient, .98). Difference between upper and lower thirds was not statistically significant ($P<.03$). Surgeon deemed all samples normal on visual inspection, but more than half fell below 50% on picrosirius scale.

of surgery and used for reattachment. Picrosirius red stain showed minimal areas of organized type I collagen and a relatively green hue, suggestive of structurally weak type III collagen in the tendon (Figure 6B). The OCT images suggest that no significant intensity variation in back-reflection occurs when the polarization state is rotated (Figure 6A). Again, this sample appeared normal and was deemed appropriate for reattachment, but OCT and histopathology showed a sample severely depleted of collagen.

In Figure 7, trichrome-stained sections are consistent with fibrocartilage, and picrosirius red stain shows lack of organized collagen bundles, even though collagen was abundant (Figures 7B, 7C). OCT images showed essentially no change in image with rotation, consistent with poorly organized collagen in this section deemed normal by visual inspection (Figure 7A). Similar results are shown in Figure 8.

Figure 9 is a plot of collagen intensity measured by picrosirius red stain against amount of change in OCT image intensity with change in incident polarization. There is a linear correlation, a correlation coefficient of .98, and the difference between upper and lower thirds was statistically significant ($P<.03$). Most interesting is that the surgeon deemed all the samples normal, but more than half fell below 50% on the picrosirius scale.

DISCUSSION

RCR is one of the most common orthopedic procedures. Unfortunately, 25% to 60% of repaired RCTs rerupture within 2 years, which represents substantial morbidity. The reason for the high failure rate is not well understood, but poor regeneration at the bone–tendon interface represents the most common pathologic finding. In this article, we have introduced a tool for studying the pathophysiology in vivo through PS-OCT.

When performing RCR, the surgeon relies mainly on the visual appearance of the tendon and prior experience. However, structurally weak collagen-depleted tendon is often used at the reattachment site, leading to reduced tensile strength of the tendon–enthesis interface. Further, it is not unreasonable to hypothesize that maintenance of some degree of tendon integrity is needed to allow migration of cells from adjacent bone. This is supported by the fact that time to repair influences outcomes, which would not likely be associated with a reduction in available regenerative cells or, alternatively, a significantly different suture technique. Therefore, it is hypothesized that repair outcomes would likely improve if the surgeon were to resect structurally weak tendon through appropriate guidance and reattach highly organized tendon. Results from this small study showed that, in more than 50% of the cases, collagen organization was abnormal by histopathology. Although this pilot study focused on an experimental and potential clinical tool, its data raise concerns and may explain in part the high rate of reattachment failures for RCR.

Another major finding was that PS-OCT identified unorganized and depleted collagen in supraspinatus tendons intended for reattachment, despite their being deemed normal on visual inspection. Histopathology showed a strong correlation with this finding and with the ability of PS-OCT to assess properties of nontransparent tissue collagen—suggesting it is feasible that intraoperative single-detector PS-OCT can be used to identify collagen-depleted tendon.

In terms of limitations, we acknowledge that the data pool was small, as it was intended to demonstrate a technology, and much larger data sets are required to develop improved scoring systems. This was not an outcome study; although the technology was demonstrated, the results were not correlated with clinical outcomes. These data represent an in vitro study, and the results need to be refined before they are adequate for in vivo clinical outcome studies.

Conclusion

We have introduced a new technology for assessing RCT collagen content and organization with the aim of ultimately improving the success rates of RCRs and understanding the causes of RCR failures. Our study results showed that PS-OCT changes in the supraspinatus tendon correlate well with histopathology. Furthermore, results in this small population showed that, in approximately 50% of cases, the tendon was normal on visual inspection but abnormal according to PS-OCT and histopathology. Long-term studies are needed to strengthen correlated imaging data with histopathology and clinical outcomes of RCRs to further evaluate the usefulness of PS-OCT–assisted assessment of RCT during RCRs.

Authors' Disclosure Statement

References

1. Oh LS, Wolf BR, Hall MP, Levy BA, Marx RG. Indications for rotator cuff repair: a systematic review. *Clin Orthop.* 2007;(455):52-63.
2. Yamaguchi K, Ditsios K, Middleton WD, Hildebolt CF, Galatz LM, Teefey SA. The demographic and morphological features of rotator cuff disease: a comparison of asymptomatic and symptomatic shoulders. *J Bone Joint Surg Am.* 2006;88(8):1699-1704.
3. Milgrom C, Schaffler M, Gilbert S, van Holsbeeck M. Rotator-cuff changes in asymptomatic adults. The effect of age, hand dominance and gender. *J Bone Joint Surg Br.* 1995;77(2):296-298.
4. Duckworth DG, Smith KL, Campbell B, Matsen FA III. Self-assessment questionnaires document substantial variability in the clinical expression of rotator cuff tears. *J Shoulder Elbow Surg.* 1999;8(4):330-333.
5. Zanetti M, Jost B, Hodler J, Gerber C. MR imaging after rotator cuff repair: full-thickness defects and bursitis-like subacromial abnormalities in asymptomatic subjects. *Skeletal Radiol.* 2000;29(6):314-319.
6. Matsen FA III, Boileau P, Walch G, Gerber C, Bicknell RT. The reverse total shoulder arthroplasty. *J Bone Joint Surg Am.* 2007;89(3):660-667.
7. Werner CM, Steinmann PA, Gilbart M, Gerber C. Treatment of painful pseudoparesis due to irreparable rotator cuff dysfunction with the Delta III reverse-ball-and-socket total shoulder prosthesis. *J Bone Joint Surg Am.* 2005;87(7):1476-1486.
8. Zumstein MA, Jost B, Hempel J, Hodler J, Gerber C. The clinical and structural long-term results of open repair of massive tears of the rotator cuff. *J Bone Joint Surg Am.* 2008;90(11):2423-2431.
9. Chard MD, Hazleman R, Hazleman BL, King RH, Reiss BB. Shoulder disorders in the elderly: a community survey. *Arthritis Rheum.* 1991;34(6):766-769.
10. Cofield RH, Parvizi J, Hoffmeyer PJ, Lanzer WL, Ilstrup DM, Rowland CM. Surgical repair of chronic rotator cuff tears. A prospective long-term study. *J Bone Joint Surg Am.* 2001;83(1):71-77.
11. Ellman H. Surgical treatment of rotator cuff rupture. In: Watson MS, ed. *Surgical Disorders of the Shoulder.* London, UK: Churchill Livingstone; 1991:283-291.
12. Braun J, Khan MA, Sieper J. Enthesitis and ankylosis in spondyloarthropathy: what is the target of the immune response? *Ann Rheum Dis.* 2000;59(12):985-994.
13. Sano H, Ishii H, Trudel G, Uhthoff HK. Histologic evidence of degeneration at the insertion of 3 rotator cuff tendons: a comparative study with human cadaveric shoulders. *J Shoulder Elbow Surg.* 1999;8(6):574-579.
14. Uhthoff HK, Sano H. Pathology of failure of the rotator cuff tendon. *Orthop Clin North Am.* 1997;28(1):31-41.
15. Blevins FT, Djurasovic M, Flatow EL, Vogel KG. Biology of the rotator cuff tendon. *Orthop Clin North Am.* 1997;28(1):1-16
16. Liem D, Lichtenberg S, Magosch P, Habermeyer P. Magnetic resonance imaging of arthroscopic supraspinatus tendon repair. *J Bone Joint Surg Am.* 2007;89(8):1770-1776.
17. Galatz LM, Ball CM, Teefey SA, Middleton WD, Yamaguchi K. The outcome and repair integrity of completely arthroscopically repaired large and massive rotator cuff tears. *J Bone Joint Surg Am.* 2004;86(2):219-224.
18. Lafosse L, Brozska R, Toussaint B, Gobezie R. The outcome and structural integrity of arthroscopic rotator cuff repair with use of the double-row suture anchor technique. *J Bone Joint Surg Am.* 2007;89(7):1533-1541.
19. Wakitani S, Goto T, Pineda SJ, et al. Mesenchymal cell-based repair of large, full-thickness defects of articular cartilage. *J Bone Joint Surg Am.* 1994;76(4):579-592.
20. Wang WG, Lou SQ, Ju XD, Xia K, Xia JH. In vitro chondrogenesis of human bone marrow–derived mesenchymal progenitor cells in monolayer culture: activation by transfection with TGF-beta2. *Tissue Cell.* 2003;35(1):69-77.
21. Koike Y, Trudel G, Uhthoff HK. Formation of a new enthesis after attachment of the supraspinatus tendon: a quantitative histologic study in rabbits. *J Orthop Res.* 2005;23(6):1433-1440.
22. Silva MJ, Ritty TM, Ditsios KT, et al. Tendon injury response: assessment of biomechanical properties, tissue morphology and viability following flexor digitorum profundus tendon resection. *J Orthop Res.* 2004;22(5):990-7.
23. Tearney GJ, Brezinski ME, Bouma BE, et al. In vivo endoscopic optical biopsy with optical coherence tomography. *Science.* 1997;276(5321):2037-2039.
24. Green LB, Pietrobon R, Paxton E, Higgins LD, Fithian D. Sources of variation in readmission rates, length of stay, and operative time associated with rotator cuff surgery. *J Bone Joint Surg Am.* 2003;85(9):1784-1789.
25. Gladstone JN, Bishop JY, Lo IK, Flatow EL. Fatty infiltration and atrophy of the rotator cuff do not improve after rotator cuff repair and correlate with poor functional outcome. *Am J Sports Med.* 2007;35(5):719-728.

26. Goutallier D, Postel JM, Bernageau J, Lavau L, Voisin MC. Fatty infiltration of disrupted rotator cuff muscles. *Rev Rhum Engl Ed.* 1995;62(6):415-422.
27. Brezinski ME. *Optical Coherence Tomography: Principles and Applications.* Burlington, MA: Academic Press; 2006.
28. Brezinski ME, Tearney GJ, Bouma BE, et al. *Optical coherence tomography for optical biopsy.* Properties and demonstration of vascular pathology. *Circulation.* 1996;93(6):1206-1213.
29. Drexler W, Stamper D, Jesser C, et al. Correlation of collagen organization with polarization sensitive imaging of in vitro cartilage: implications for osteoarthritis. *J Rheumatol.* 2001;28(6):1311-1318.
30. Roberts MJ, Adams SB Jr, Patel NA, et al. A new approach for assessing early osteoarthritis in the rat. *Anal Bioanal Chem.* 2003;377(6):1003-1006.
31. Rogowska J, Patel NA, Fujimoto JG, Brezinski ME. Optical coherence tomographic elastography technique for measuring deformation and strain of atherosclerotic tissues. *Heart.* 2004;90(5):556-562.
32. Rogowska J, Patel N, Plummer S, Brezinski ME. Quantitative optical coherence tomographic elastography: method for assessing arterial mechanical properties. *Br J Radiol.* 2006;79(945):707-711.
33. Schmitt J. OCT elastography: imaging microscopic deformation and strain of tissue. *Optics Express.* 1998;3(6):199-211.
34. Adams SB Jr, Herz PR, Stamper DL, et al. High-resolution imaging of progressive articular cartilage degeneration. *J Orthop Res.* 2006;24(4):708-715.
35. Liu B, Harman M, Giattina S, et al. Characterizing of tissue microstructure with single-detector polarization-sensitive optical coherence tomography. *Appl Opt.* 2006;45(18):4464-4479.
36. Li X, Martin S, Pitris C, et al. High-resolution optical coherence tomographic imaging of osteoarthritic cartilage during open knee surgery. *Arthritis Res Ther.* 2005;7(2):R318–R323.
37. Kumagai J, Uhthoff HK, Sarkar K, Murnaghan JP. Collagen type III in rotator cuff tears: an immunohistochemical study. *J Shoulder Elbow Surg.* 1992;1(4):187-192.
38. Junqueira LC, Assis Figueiredo MT, Torloni H, Montes GS. Differential histologic diagnosis of osteoid. A study on human osteosarcoma collagen by the histochemical picrosirius-polarization method. *J Pathol.* 1986;148(2):189-196.
39. Junqueira LC, Bignolas G, Brentani RR. Picrosirius staining plus polarization microscopy, a specific method for collagen detection in tissue sections. *Histochem J.* 1979;11(4):447-455.
40. Itoi E, Minagawa H, Sato T, Sato K, Tabata S. Isokinetic strength after tears of the supraspinatus tendon. *J Bone Joint Surg Br.* 1997;79(1):77-82.
41. Itoi E, Hsu HC, Carmichael SW, Morrey BF, An KN. Morphology of the torn rotator cuff. *J Anat.* 1995;186(pt 2):429-434.
42. Huang D, Swanson EA, Lin CP, et al. Optical coherence tomography. *Science.* 1991;254(5035):1178-1181.
43. Herrmann JM, Pitris C, Bouma BE, et al. High resolution imaging of normal and osteoarthritic cartilage with optical coherence tomography. *J Rheumatol.* 1999;26(3):627-635.
44. Martin SD, Patel NA, Adams SB Jr, et al. New technology for assessing microstructural components of tendons and ligaments. *Int Orthop.* 2003;27(3):184-189.
45. Zheng K, Martin SD, Rashidifard CH, Liu B, Brezinski ME. In vivo micronscale arthroscopic imaging of human knee osteoarthritis with optical coherence tomography: comparison with magnetic resonance imaging and arthroscopy. *Am J Orthop (Belle Mead, NJ).* 2010;39(3):122-125.
46. Shortkroff S, Goodwin A, Giattina S, Liu B, Brezinski ME. Use of formalin-fixed tissues for ex vivo imaging with optical coherence tomography (OCT). In: *Imaging, Manipulation, and Analysis of Biomolecules, Cells, and Tissues IV.* San Jose, CA: Society of Photo-Optical Instrumentation Engineers; 2006.
47. Dayan D, Hiss Y, Hirshberg A, Bubis JJ, Wolman M. Are the polarization colors of picrosirius red–stained collagen determined only by the diameter of the fibers? *Histochemistry.* 1989;93(1):27-29.

ERRATUM

In the article, "Lumbar Extracavity Corpectomy With a Single Stage Circumferential Arthrodesis: Surgical Technique and Clinical Series" (*Am J Orthop.* 2012;41(7):316-320), 2 figures were printed incorrectly (Figures 4 and 5). Consequently, both figures are reprinted below in their corrected form. The *American Journal of Orthopedics®* makes every possible effort to ensure accuracy in its articles and apologizes for the mistake.

Figure 4. An expandable interbody cage is placed parallel to the exiting L3 and L4 nerve roots as marked by the 2 k-wires. Note that the cage is perpendicular to the dural sac while it is advanced into corpectomy defect.
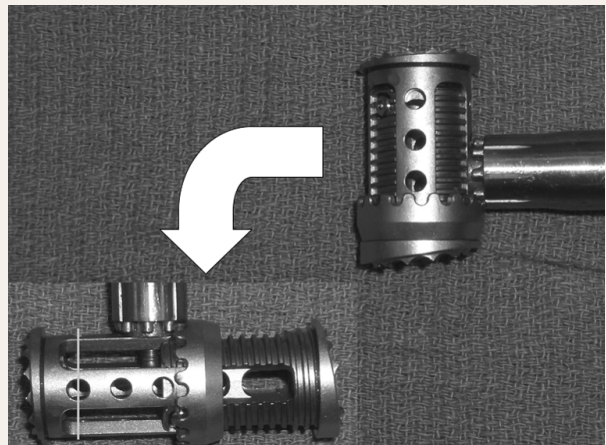

Figure 5. The cage is then rotated 90° within the corpectomy site and expanded as demonstrated by the photograph.